INTRODUCTION

heumatoid arthritis (RA) is a chronic systemic inflammatory disease of unknown etiology, which primarily affects the synovia; where the persisting synovitis of symmetric peripheral joints can lead to structural damage of cartilage, bones, tendons, and ligaments (*Ivanac et al.*, 2015).

The disease affects approximately 1% of the world's population (Rowbotham et al., 2011).

Since there is no single test to diagnose RA, clinicians use a number of tests to support the clinical diagnosis. This traditionally includes rheumatoid factor (RF), anticitrullinated peptide (anti-CCP), erythrocyte sedimentation rate (ESR), and/or serum C-reactive protein (CRP) levels as well as imaging using radiographs of the hands, wrists, and feet (Farng and Friedrich, 2011).

Radiographs have traditionally been the mainstay for imaging patients with rheumatoid arthritis; with findings such as soft-tissue swelling, periarticular osteopenia, joint space loss, joint subluxation, and marginal erosions considered features that are commonly seen. However, information regarding the synovium is much more difficult to assess on radiographs (Rowbotham et al., 2011).

Hence, despite plain conventional radiography being the most frequently used method to diagnose the bone and joint



erosions, its main drawback have always been the inability to predict the soft tissue lesions in the early stage of the disease (Snekhalatha et al., 2016).

Up till recent advances in medical management of rheumatoid arthritis, radiographic diagnosis and follow-up of the condition were considered adequate, however, with the increasing use of disease-modifying antirheumatic drugs, early diagnosis is now of paramount importance and disease progression is assessed regularly to monitor efficacy of the treatment. This called for the development of new methods for imaging early joint affection in cases of RA (Rowbotham et al., 2011).

A recent tool used for assessment of rheumatological joint affection is the ultrasonography (US) using high frequency probes, with high resolution gray-scale that enables accurate visualization of the inflamed synovia, joint fluid, and para articular changes. Several studies have also shown that color and power Doppler enables excellent visualization of blood flow in inflamed joints, allowing for estimating the stage of inflammatory changes by analyzing the synovial thickening and reduction of vascularization (Rizzo et al., 2013).

Some authors have argued that targeting the therapy to power Doppler US (PDUS) based activity may provide better outcomes compared with targeting therapy to clinical targets alone, the thing that renders it an attractive and feasible marker of disease activity in RA (Wakefield et al., 2012).

AIM OF THE WORK

o evaluate the utility of high resolution ultrasound with color duplex-Doppler as an imaging-based biomarker for activity in cases of clinico-laboratory active RA of the small joints.

Chapter 1

ANATOMY OF THE WRIST AND HAND JOINTS

The wrist joint is considered to be the most complex articulation in the human body. However, its anatomy can be simplified into three major compartments: the distal radioulnar joint (DRUJ), the radiocarpal joint, and the midcarpal joint; they often intercommunicate through a common synovial cavity (*Thomas et al.*, 2008).

Bones of the wrist (Carpus): The carpus contains eight bones in proximal and distal rows of four. Proximally, in lateral to medial order, are the scaphoid, lunate, triquetral and pisiform; in the distal row is the trapezium, trapezoid, capitate and hamate (Fig. 1), (Fig.2). The scaphoid, lunate and triquetral bones form an arch proximally convex, articulating with the radius and articular disc of the inferior radioulnar joint. The arch's concavity is a distal recess embracing, proximally, the projecting aspects of the capitate and hamate; the two rows are thus mutually and firmly adapted (*Roger*, 2015).

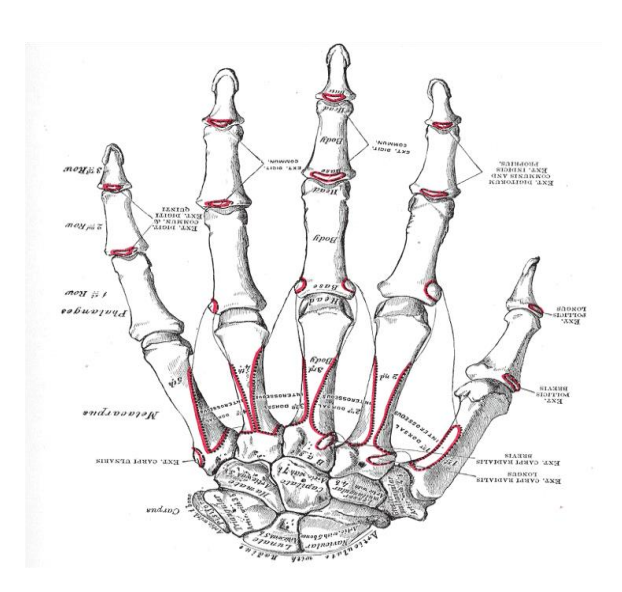


Fig. (1): Bones of the left hand from the dorsal aspect (Quoted from Standring, 2010).

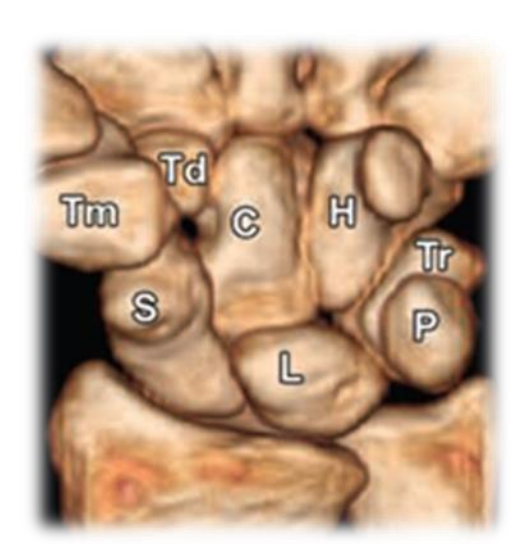


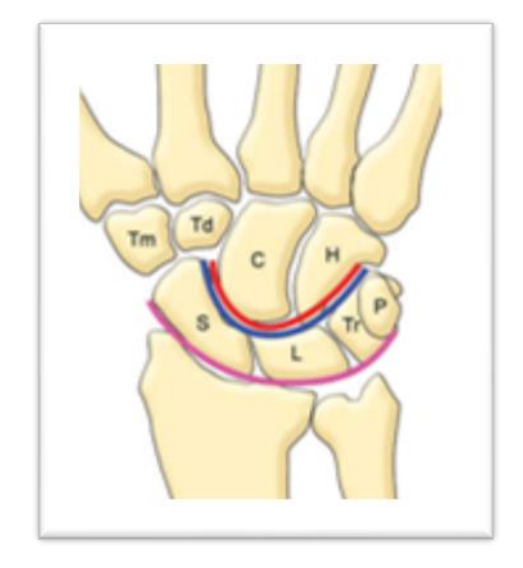
Fig. (2): Carpal anatomy, three-dimensional (3D) CT images show the normal wrist. C = apitates, H = hamate, L = lunate, P = pisiform, S = scaphoid, Td = trapezoid, Tm = trapezium, Tr = triquetrum (*Quoted from Rathachai et al.*, 2008).

Carpal arcs (Gilula arcs or lines) are three smooth arcs: (Fig. 3)

- **Arc I** outlines the proximal surface of the scaphoid, lunate, and triquetrum.
- **Arc II** represents the smooth arc that defines the distal surface of these same three carpal bones.
- **Arc III** outlines the proximal surface of the capitate and hamate.

The continuity of the carpal arcs should be assessed on all frontal wrist radiographs. Disruption of one of these arcs suggests an abnormality at that site. In the evaluation of the neutral lateral radiograph, a normal coaxial alignment of the radius, lunate, and capitate should be expected (*Rathachai et al.*, 2008).

Fig. (3): Normal anatomy of the carpal bones. Diagram of the wrist (frontal view) shows the eight carpal bones and the three carpal arcs (Gilula arcs), which are shown as pink (arc I), blue (arc II), and red (arc III) lines. C = capitate, H = hamate, L = lunate, P = pisiform, S = scaphoid, Tm = trapezium, Td = trapezoid, Tr = Triquetrum (Quoted from Rathachai et al., 2008).



The wrist (radiocarpal) joint (Fig. 4):

It is a synovial biaxial and ellipsoid joint (*Standring*, 2010).

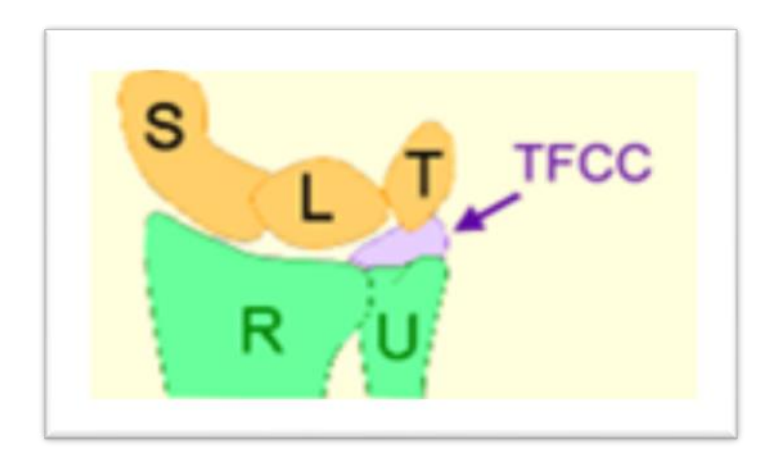


Fig. (4): Radiocarpal joint; TFCC (triangular fibro-cartilage complex) (*Quoted from Neumann, 2015*).

1. Articular surfaces:

The convex proximal surface of the carpus (formed by the scaphoid, lunate and triquetrum bones and their interosseous ligaments), and the concave socket formed by the distal surfaces of the radius and the triangular articular disc. This disc joins the medial edge of the articular surface of radius to the styloid process of ulna, separating the ulna from the joint (*Romanes*, 2010).

2. Fibrous capsule and synovial membrane:

The capsule passes from the margins of distal ends of radius and ulna, and from the margins of the articular disc to

the proximal row of carpal bones, excluding the pisiform bone (*Romanes*, 2010). The capsule is strengthened by palmar radiocarpal and ulnocarpal, dorsal radiocarpal and radial and ulnar collateral ligaments, the synovial membrane lines the fibrous capsule, separate from that of distal radioulnar and intercarpal joints (*Standring*, 2010).

3. Tendons:

The tendons of the wrist are grouped into flexor and extensor compartments (*Joseph et al.*, 2011).

A- Extensor tendons:

The extensor tendons are divided into six compartments on the dorsal aspect of the wrist and are sequentially numbered from the radial to the ulnar side (**Fig.5**). These tendons lie superficial to the carpal bones and interosseous ligaments (*Joseph et al.*, 2011).

The first compartment is located lateral to the distal radius and contains the abductor pollicis longus and extensor pollicis brevis tendons. The second compartment is located lateral to Lister's tubercle, an osseous protuberance on the dorsal distal radius, and contains the extensor carpi radialis brevis and longus tendons. The third compartment is located medial to Lister's tubercle and contains the extensor pollicus longus tendon. The fourth extensor compartment contains the extensor indicis proprius and extensor digitorum communis

tendons, and **the fifth** compartment contains the extensor digiti minimi tendon. **The sixth** compartment, located medial to the ulnar styloid, contains the extensor carpi ulnaris tendon (*Joseph et al.*, 2011).

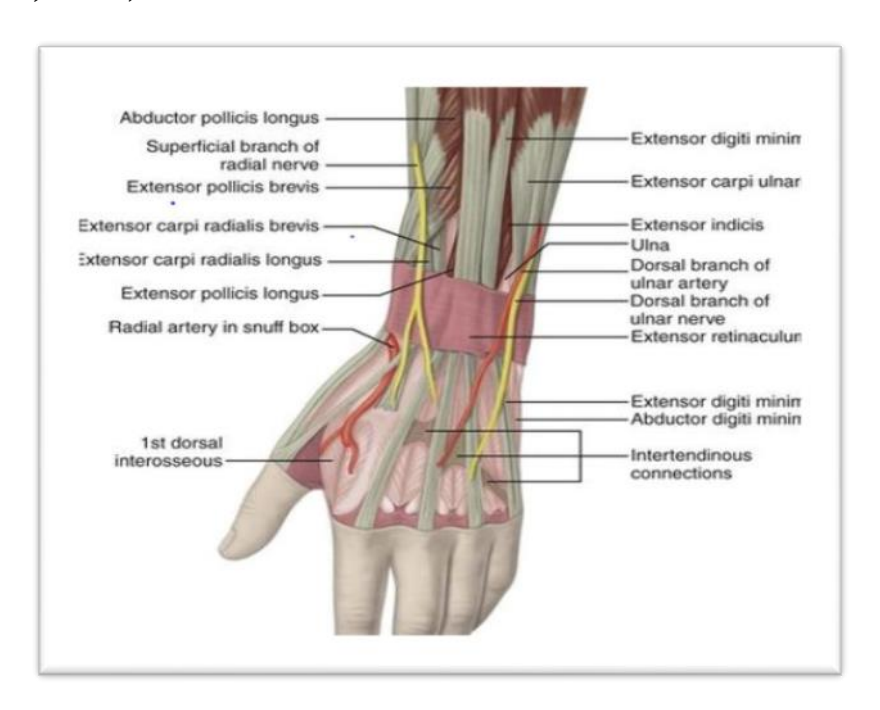


Fig. (5): Extensor Tendons with the Six Tendon Sheath Compartments (Dorsum of the Wrist) (*Quoted from Joseph et al.*, 2011).

B- Flexor tendons:

The flexor tendons, which begin in the distal forearm, are located on the volar aspect of the wrist and reside either within or adjacent to the carpal tunnel (**Fig. 6**). The flexor pollicis longus is dorsal and lateral to the median nerve. It inserts on the distal phalanx of the thumb and is enveloped by the radial bursa (*Ham et al.*, 2015).

The flexor digitorum superficialis and profundus tendons reside medial to the median nerve, enveloped by the ulnar bursa. The flexor carpi radialis tendon is located outside the carpal tunnel, coursing just lateral to the tunnel, and inserts on the base of the second metacarpal bone. The flexor carpi ulnaris tendon is located medial to the ulnar nerve and inserts principally on the pisiform but with fibers extending to the humulus and the base of the fourth and fifth metacarpal bones (*Anderson et al.*, 2012).

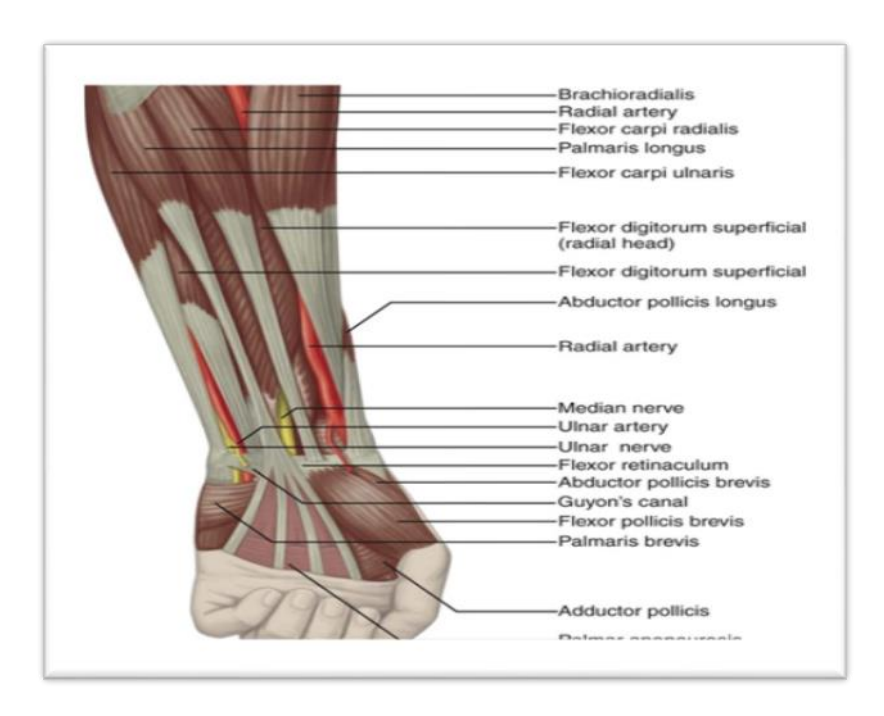


Fig. (6): Wrist flexors (Quoted from David et al., 2014).

4. Ligaments of the wrist:

They are either situated between the fibrous and synovial layers of the wrist joint, termed intracapsular, or lying

superficial to the fibrous layers, those are extracapsular, in addition to the flexor and extensor retinacula and the pisotriquetral ligament (*Standring*, 2010). Intracapsular ligaments are further subdivided into either intrinsic (between carpal bones alone) or extrinsic (between carpal and metacarpal bones or between carpal bones and the radius and/or ulna) (*Theumann et al.*, 2013).

A- Volar extrinsic ligaments:

The most functionally significant of the extrinsic ligaments are the volar radiocarpal ligaments (Fig.7). These ligaments are the most important stabilizers of wrist motion (*Michael & Joel, 2016*).

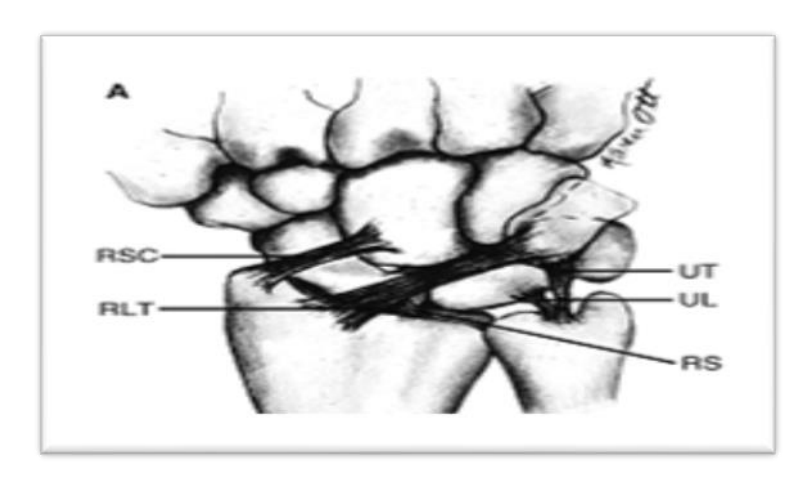


Fig. (7): Diagram illustrating the volar radiocarpal and ulnocarpal ligaments. RLT, radiolunatotriquetral ligament; RSC, radioscaphocapitate ligament; UL, ulnolunate ligament; UT, ulnotriquetral ligament (*Quoted from Michael & Joel, 2016*).

B- Dorsal extrinsic Ligaments:

There are two main ligaments at the dorsum of the wrist that make a lateral V shaped configuration, the dorsal radiocarpal ligament and the dorsal intercarpal ligament (**Fig. 8**) (*Anastasios et al.*, 2015).

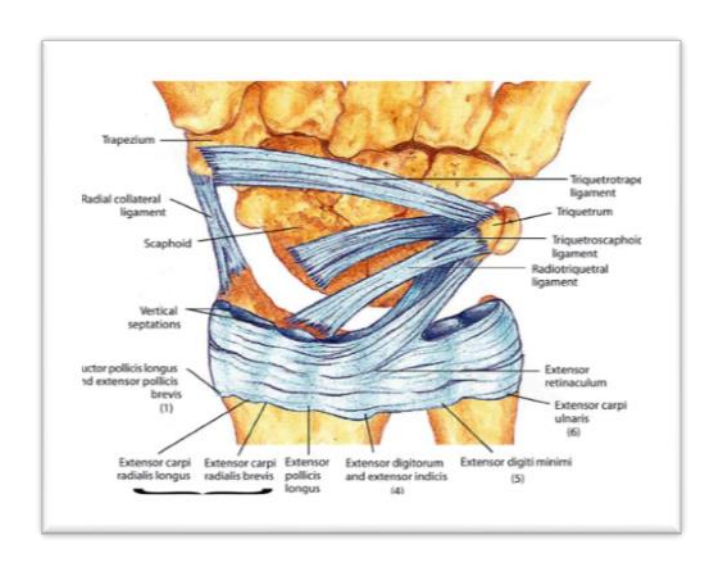


Fig. (8): Diagram illustrates the extensor retinaculum and dorsal carpal ligaments (*Quoted from Standring*, 2010).

C- Intrinsic ligaments:

They are stronger and shorter than extrinsic ligaments. Rupture of one or more of them leads to clinical instability of the carpus (**Fig. 9**); they are:

a- Proximal row interosseous ligaments: as the scapholunate and lunotriquetral.

- b- Distal row interosseous ligaments: between the capitate, hamate, trapezium and trapezoid.
- c- Palmar midcarpal ligament.
- d- Dorsal midcarpal ligament (Standring, 2010).

It is the general belief that the scapholunate ligament and lunotriquetral ligament are the most important intrinsic ligaments for carpal stability (*Theumann et al., 2013*).

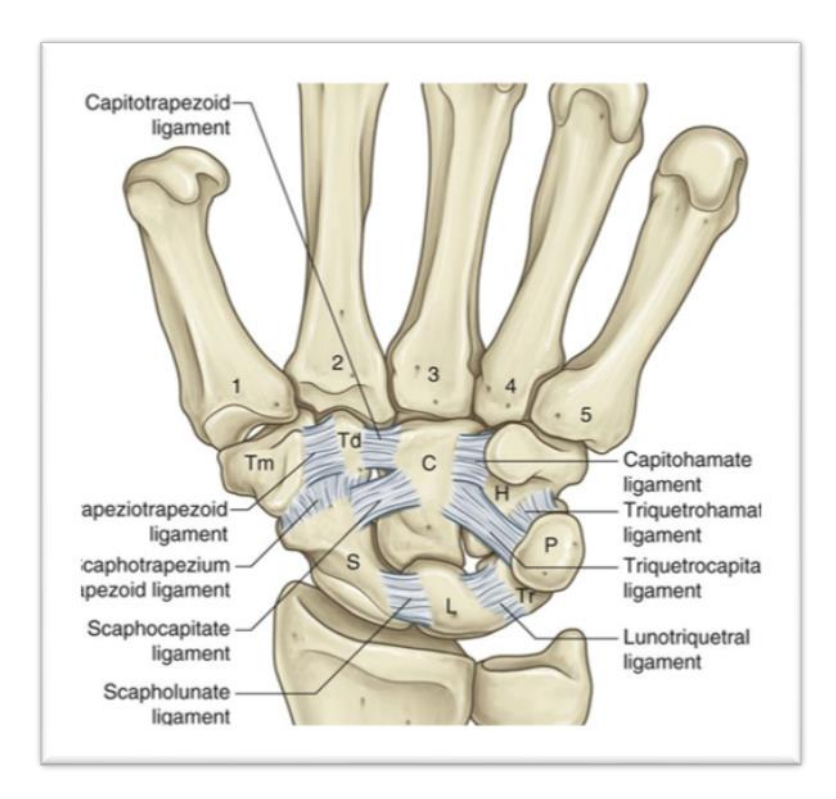


Fig. (9): Intrinsic ligament of the wrist (Quoted from Theumann et al., 2013).

5. Nerve supply:

The posterior interosseous (radial) and anterior interosseous (median) nerves (*Sinnatamby*, 2007).

Distal radioulnar joint:

The distal radioulnar joint is formed by the head of ulna and the segmoid notch of radius (**Figs. 10, 11**). This joint is separated from the radiocarpal joint by an articular disc lying between the radius and the styloid process of ulna (*Platzer and Werner, 2008*).



Fig. (10): Distal radioulnar, radiocarpal, and mid carpal joints (Quoted from Neumann, 2015).

DISTAL RADIOULNAR JOINT

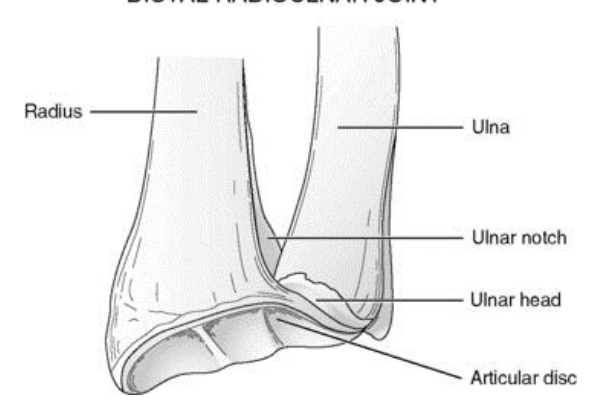


Fig. (11): The articular surface of the distal end of the radius and the adjacent triangular cartilage are exposed by removal of the carpal bones (*Quoted from Standring*, 2010).

The intercarpal joints (Fig. 12):

They are synovial plane joints between the individual bones of the proximal row of the carpus; between the individual bones of the distal row of the carpus and finally, **the midcarpal joint**, between the proximal and distal rows of carpal bones, the fibrous capsule surrounds each joint, and it is lined with synovial membrane (**Fig. 12**) The carpal bones are united together by strong anterior, posterior and interosseous ligaments. Movements allowed are small degrees of gliding movements (*Snell*, 2011).